

RESEARCH

Open Access



The novel circFKBP8/miR-432-5p/E2F7 cascade functions as a regulatory network in breast cancer

Zhongkui Jin¹, Wang Xu¹, Kunlin Yu¹, Cailu Luo¹, Xiaodan Luo¹, Tao Lian¹ and Changshan Liu^{1*}

Abstract

Background Circular RNAs (circRNAs) are capable of affecting breast cancer (BC) development. However, the role and underneath mechanism of circFKBP8 (also known as hsa_circ_0000915) in BC remain largely unknown.

Methods Expression analyses were performed using quantitative real-time polymerase chain reaction (qRT-PCR), western blot, and immunohistochemistry (IHC) assays. Effects on cell functional phenotypes were determined by assessing cell proliferation, migratory capacity, invasion, and stemness in vitro. The relationship between microRNA (miR)-432-5p and circFKBP8 or E2F transcription factor 7 (E2F7) was examined by RNA pull-down, dual-luciferase reporter, and RNA immunoprecipitation (RIP) assays. Xenograft assays were used to identify the function of circFKBP8 in vivo.

Results CircFKBP8 was presented at high levels in BC tissues and cells. High circFKBP8 expression was associated with worse overall survival in BC patients. CircFKBP8 suppression inhibited BC cell proliferation, migratory capacity, invasion and stemness in vitro. CircFKBP8 suppression blocked xenograft tumor growth in vivo. Mechanistically, circFKBP8 functioned as a miR-432-5p sponge to modulate E2F7 expression. CircFKBP8 modulated BC cell malignant behaviors by miR-432-5p, and miR-432-5p affected these cell phenotypes through E2F7.

Conclusion Our observations prove that circFKBP8 promotes BC malignant phenotypes through the miR-432-5p/E2F7 cascade, offering a promising therapeutic and prognostic target for BC.

Highlights

- CircFKBP8 and E2F7 are notably upregulated, and miR-432-5p is downregulated in breast cancer and cells.
- CircFKBP8 suppression inhibits proliferation, migration, invasion, and stemness of breast cancer cells.
- CircFKBP8 regulates breast cancer progression through the miR-432-5p/E2F7 axis.
- CircFKBP8 accelerates tumor growth in vivo.

Keywords circFKBP8, miR-432-5p, E2F7, Breast cancer

*Correspondence:

Changshan Liu
lccvylc@163.com

¹Department of Breast Surgery, Yichun People's Hospital & The Affiliated Yichun Hospital of Nanchang University, No.1061 Jinxu avenue, Yiyang New District 336000, Yichun, Jiangxi, China



© The Author(s) 2024. **Open Access** This article is licensed under a Creative Commons Attribution 4.0 International License, which permits use, sharing, adaptation, distribution and reproduction in any medium or format, as long as you give appropriate credit to the original author(s) and the source, provide a link to the Creative Commons licence, and indicate if changes were made. The images or other third party material in this article are included in the article's Creative Commons licence, unless indicated otherwise in a credit line to the material. If material is not included in the article's Creative Commons licence and your intended use is not permitted by statutory regulation or exceeds the permitted use, you will need to obtain permission directly from the copyright holder. To view a copy of this licence, visit <http://creativecommons.org/licenses/by/4.0/>. The Creative Commons Public Domain Dedication waiver (<http://creativecommons.org/publicdomain/zero/1.0/>) applies to the data made available in this article, unless otherwise stated in a credit line to the data.

Introduction

Breast cancer (BC) is a serious malignant tumor with significant incidence and mortality among women worldwide [1, 2]. With the deterioration of lifestyle and ecological environment, the percentage of new cases of BC in China is as high as 3–4% annually [3]. Therefore, elucidating the pathogenesis of BC, controlling the incidence of BC and improving the therapeutic effect of BC have become major problems to be solved.

Unlike linear RNA, circular RNAs (circRNAs) have a closed-loop structure and are a special class of non-coding RNA, so they are conserved and tissue-specific and not easily degraded by nucleic acid exonucleases [4, 5]. Studies have shown that circRNAs are involved in the occurrence and development processes of various tumors by acting as transcription regulators or sponges of microRNAs (miRNAs) [6]. For example, circSEC24A was upregulated in pancreatic cancer (PC), and increased circSEC24A expression promoted PC progression by upregulating TGFBR2 via miR-606 [7]. Circ_0001367 was reduced in glioma, and its upregulation could enhance LUZP1 expression to inhibit glioma progression by sponging miR-545-3p [8]. Hsa_circ_0008434 was capable of promoting gastric cancer growth and metastasis via the miR-6838-5p/USP9X cascade [9]. Many studies have demonstrated that circRNAs possess critical functions in BC progression. For instance, wan et al. found that circTFF1 regulated BC progression through sponging miR-338-3p and promoting FGFR1 expression [10]. Zhong et al. revealed that circRASSF2 accelerated BC cell malignant behaviors through regulating the miR-1205/HOXA1 cascade [11]. Circ_0084927 was enriched in BC and facilitated BC progression via sponging miR-142-3p to modulate ERC1 expression [12].

According to a previous study, we found that many circRNAs were dysregulated in BC, of which circFKBP8 (also called hsa_circ_0000915 based on the circBase ID), a relatively unexplored circRNA in cancer biology, was significantly upregulated in BC [13], implying

the implication of circFKBP8 in BC progression. Furthermore, the function and underlying mechanism of circFKBP8 in BC are unclear. Therefore, we sought to explore the precise action of circFKBP8 in BC.

Materials and methods

Tissue sample

70 pairs of BC tissue specimens and adjacent non-cancer tissue specimens were obtained from BC cases with the written informed consent at Yichun People's Hospital & The Affiliated Yichun Hospital of Nanchang University. All the patients enrolled in this study had not anti-cancer therapy before operation, and their clinicopathological features were presented in Table 1. The Ethics Committee of Yichun People's Hospital & The Affiliated Yichun Hospital of Nanchang University approved this study with approval No.20,230,218.

Cells and cell culture

Four BC cells (MDA-MB-231, MDA-MB-453, MDA-MB-468, and BT549) and human normal breast cells MCF-10 A were obtained from ATCC (Manassas, VA, USA). All cells were incubated in DMEM medium (Gibco, Carlsbad, CA, USA) with 10% FBS and 1% penicillin/streptomycin. Cells were cultured in a 37°C, 5% CO₂ incubator with humidified air.

Cell transfection

For transient transfection, miR-432-5p mimic or inhibitor (miR-432-5p or inh-miR-432-5p), E2F transcription factor 7 (E2F7) overexpressed plasmid pcDNA-E2F7 (E2F7) and their negative controls (RiboBio, Guangzhou, China) were transfected into BC cells using lipofectamine 3000 reagent (Invitrogen). The transfection efficiency was detected 24 h after transfection. For stable knockdown of circFKBP8, three short hairpin RNAs (shRNAs) targeting circFKBP8 (sh-circFKBP8#1: 5'-ACAGCCCGTTCC CTGCCTTGG-3'; #2: 5'-CTCAACAGCCCGTTCCCTG CC-3'; and #3: 5'-CCCGTTCCCTGCCTTGGGGGC-3') were constructed by RiboBio and transfected into BC cells, respectively. Viral supernatants were obtained and used to infect BC cells for 48 h. To establish stable knockdown cell line of circFKBP8, virus-positive BC cells were selected by puromycin for 2 weeks.

Quantitative real-time polymerase chain reaction (qRT-PCR)

Total RNA was isolated in Trizol reagent (Invitrogen). The concentration of RNA was determined by Nano-Drop2000 (Thermo Fisher Scientific, Waltham, MA, USA). Total RNA was converted into cDNA under use of PrimeScript RT reagent kit (Exiqon, Aarhus, Denmark) with random primers and miRNA-specific primers (miR-432-5p: 5'-CTCAACTGGTGTCTGGAGTCGGCAA

Table 1 The clinicopathologic features in breast cancer patients

Parameters	N=70
Age, years	
< 50	33
≥ 50	37
Tumor size	
< 2	29
≥ 2	41
TNM stage	
I-II	55
III	15
Lymph node metastasis	
No	52
Yes	18

TTCAGTTGAGCCACCCAA-3'; miR-490-3p: 5'-CTC AACTGGTGTCTGGAGTCGGCAATTCAGTTGAG CCACCCAA-3'). The qPCR analysis was performed by SYBR Green I (Takara, Dalian, China) and specific primers. The relative RNA expression was measured by the $2^{-\Delta\Delta C_t}$ method. Primers were shown in Table 2. GAPDH (for circRNA and mRNA) and U6 (for miRNA) were used as the housekeeping genes.

RNase R treatment

Total RNA was obtained from BC cells. 2.5 μ g of RNA was cultured with 4 U of RNase R (20 U/ μ L, BioVision, Milpitas, CA, USA) at 37°C for 0.5 h. Then, circFKBP8 and GAPDH levels were detected by qRT-PCR.

CircRNA localization assay

Total RNA was isolated from the nucleus and cytoplasm of BC cells using PARIS™ Kit (Invitrogen), according to the manufacturer's instructions. Then, circFKBP8 amount was analyzed via qRT-PCR. U6 and GAPDH were used as nuclear and cytoplasmic controls, respectively.

CCK8 assay

2×10^3 BC cells were cultured in 96-well plates for 48 h. After that, 10 μ L CCK8 reagent was added into cells for additional 2 h. Then, the absorbance (450 nm) value was detected using a microplate reader (Thermo Fisher Scientific).

5-Ethynyl-29-deoxyuridine (EDU) assay

BeyoClick™ EdU-647 kit (Beyotime, Shanghai, China) was used to detect cell proliferation ability. In brief, BC cells grown in 96-well plates were incubated with 25 μ M EDU solution. After 4 h, cells were treated with paraformaldehyde and Triton X-100 (Beyotime). Subsequently, cells were incubated with 100 μ L EdU detection solution for 30 min, and cell nuclei were stained with 300 μ L diaminodiphenylindole (DAPI; Beyotime) for 20 min. Then,

pictures were taken under the fluorescence microscope and the EDU-stained cells were scored relative to total cells.

Colony formation assay

Approximately 500 BC cells were seeded into 6-well plates and incubated for 2 weeks. Then, cells were fastened with methanol (Sigma-Aldrich) for 10 min and stained with crystal violet (Sigma-Aldrich) for 15 min. The number of colonies was counted by Image J software (NIH, Bethesda, MD, USA).

Transwell assay

BC cells in serum-free DMEM medium were plated into the upper transwell chamber (Corning Inc., Corning, NY, USA) precoated with (invasion assay) or without (migration assay) matrigel (Corning Inc.), and lower chamber was added with DMEM medium plus 20% FBS. After 24 h, the migrated and invaded cells were fixed and stained by 0.1% crystal violet (Sigma-Aldrich). Pictures of cells were photographed under a microscope.

Sphere formation assay

BC cells were seeded into Ultra-low attachment 6-well plates (Corning Inc.) with DMEM medium, which included epidermal growth factor (100 ng/ml), basic fibroblast growth factor (10 ng/ml), B27 (2%), and Insulin (4 ng/ml) (Sigma-Aldrich). After ten days of culture, pictures of cells were obtained with a microscope.

Western blot

Total protein was acquired in lysis of radioimmunoprecipitation assay (RIPA) buffer (Sigma-Aldrich). 40 μ g protein was loaded for sodium dodecyl sulfate polyacrylamide gel electrophoresis (SDS-PAGE). The resulting gels were transferred to polyvinylidene fluoride membranes (Sigma-Aldrich), followed by blocking in 5% non-fat milk (Invitrogen). The primary antibodies were as follows: anti-E2F7 (1:1,000, AV37583, Sigma-Aldrich, St. Louis, MO, USA), anti-KI-67 (1:1,000, ab92742, Abcam, Cambridge, MA, USA), anti-MMP2 (1:1,000, ab86607, Abcam), anti-Nanog (1:1,000, ab190250, Abcam), and anti- β -actin (1:4,000, ab8226, Abcam). The secondary antibody (1:5,000, ab205718, Abcam) was incubated at room temperature for 1 h. The protein signals were visualized by ECL Kit (Solarbio).

Dual-luciferase reporter assay

The segments of circFKBP8 or E2F7 3'UTR covering wild-type (WT) and mutant-type (MUT) binding sites of miR-432-5p were constructed into pmirGLO vector (Promega, Madison, WI, USA). Luciferase reporter vectors and miR-432-5p mimic or miR-NC mimic were

Table 2 Primers sequences used for PCR

Name		Primers for PCR (5'-3')
circ_0000915(circFKBP8)	Forward	CCAAGGCAGGGAACGGG
	Reverse	CGTCTGCAGATGTACGGTGA
E2F7	Forward	GATCGATCAAGGATGGCCCC
	Reverse	TTCCGCTTGCTGTCTGTCAA
miR-432-5p	Forward	GTATGATCTTGGAGTAGGTCA
	Reverse	CTCAACTGGTGTCTGGAG
miR-490-3p	Forward	GTATGACAACCTGGAGGACT
	Reverse	CTCAACTGGTGTCTGGAG
GAPDH	Forward	GGAGCGAGATCCCTCCAAAAT
	Reverse	GGCTGTTGTCATCTTCTCATGG
U6	Forward	CTCGCTTCGGCAGCACA
	Reverse	AACGCTTCACGAATTTGCGT

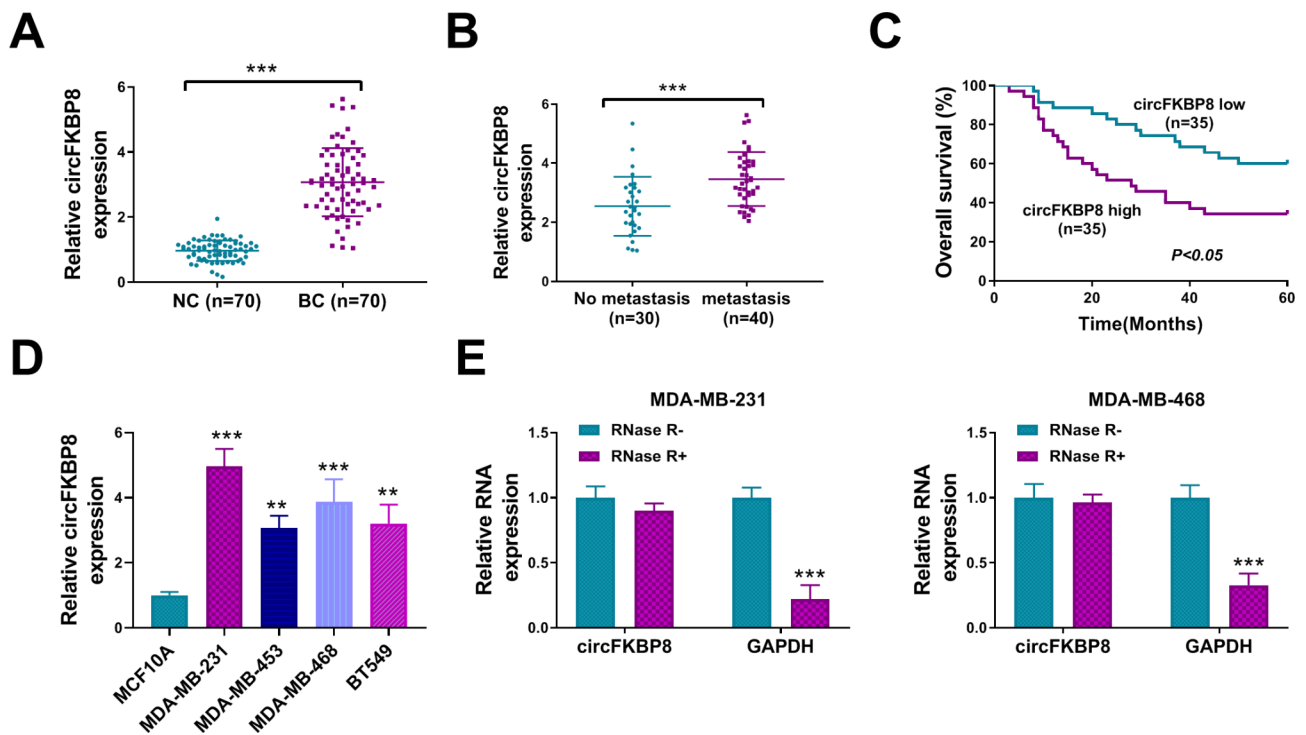


Fig. 1 CircFKBP8 was highly expressed in BC. **(A)** CircFKBP8 expression was detected by qRT-PCR in BC tissues ($n=70$) and adjacent non-cancer tissues (NC) ($n=70$); **(B)** circFKBP8 expression in BC patients with no metastasis and distant metastasis; **(C)** The prognostic value of circFKBP8 by survival curve analysis; **(D)** circFKBP8 expression in BC cells (MDA-MB-231, MDA-MB-453, MDA-MB-468, and BT549) and human normal breast cells MCF-10 A; **(E)** The expression of circFKBP8 and GAPDH was detected after treatment with or without RNase R in BC cells. ** $P < 0.01$, *** $P < 0.001$

co-transfected into BC cells through lipofectamine 3000 reagent. 48 h later, luciferase activities were analyzed.

RNA pull-down assay

C-1 magnetic beads (Life Technologies, Carlsbad, CA, USA) were pre-treated with oligo probe or circFKBP8 probe (Ribobio) for 2 h. Total extractions of MDA-MB-231 and MDA-MB-468 cells were incubated with the probe-bead complex at 4°C overnight. Then, miR-490-3p and miR-432-5p levels were detected using qRT-PCR.

RNA immunoprecipitation (RIP) assay

RIP assay was conducted by the RIP Kit (Genesee, Guangzhou, China). In brief, BC cell lysates were mixed with the magnetic beads labeled with anti-Ago2 (ab156780, Abcam) or anti-IgG (ab109489, Abcam) antibody for 12 h. After beads were digested by proteinase K, the enrichment levels of miR-432-5p and circFKBP8 were evaluated by qRT-PCR.

Tumor xenografts assay

Stable MDA-MB-231 cells (5×10^6 cells/ 0.2 mL PBS) with knockdown of circFKBP8 (sh-circFKBP8#1) or shRNA negative control group (sh-NC) were injected subcutaneously into BALB/c nude mice (6-week-old, $n=5$ /group). Tumor volume was measured every 7 days

using the formula: $\text{volume} = (\text{length} \times \text{width}^2) / 2$. After 35 days, tumors were isolated from the sacrificed mice and weighted. The excised tumors were also used to detect the protein levels of E2F7 (ab245655, Abcam), KI-67 (ab15580, Abcam), MMP2 (ab97779, Abcam), and Nanog (ab109250, Abcam) by Immunohistochemistry (IHC). All experiments in nude mice were approved by Animal Ethical Committee of The Ethics Committee of Yichun People's Hospital & The Affiliated Yichun Hospital of Nanchang University approved this study with approval No.20,230,218.

Statistical analysis

The results were expressed as mean \pm standard deviation (SD). All assays were independently performed with three times. Graphpad Prism 8.0 software was used to analyze data. Two group differences were analyzed by Student's *t*-test or Wilcoxon signed-rank test. The multiple groups were compared by one-way analysis of variance with Kruskal-Wallis tests. $P < 0.05$ was defined as statistical significance.

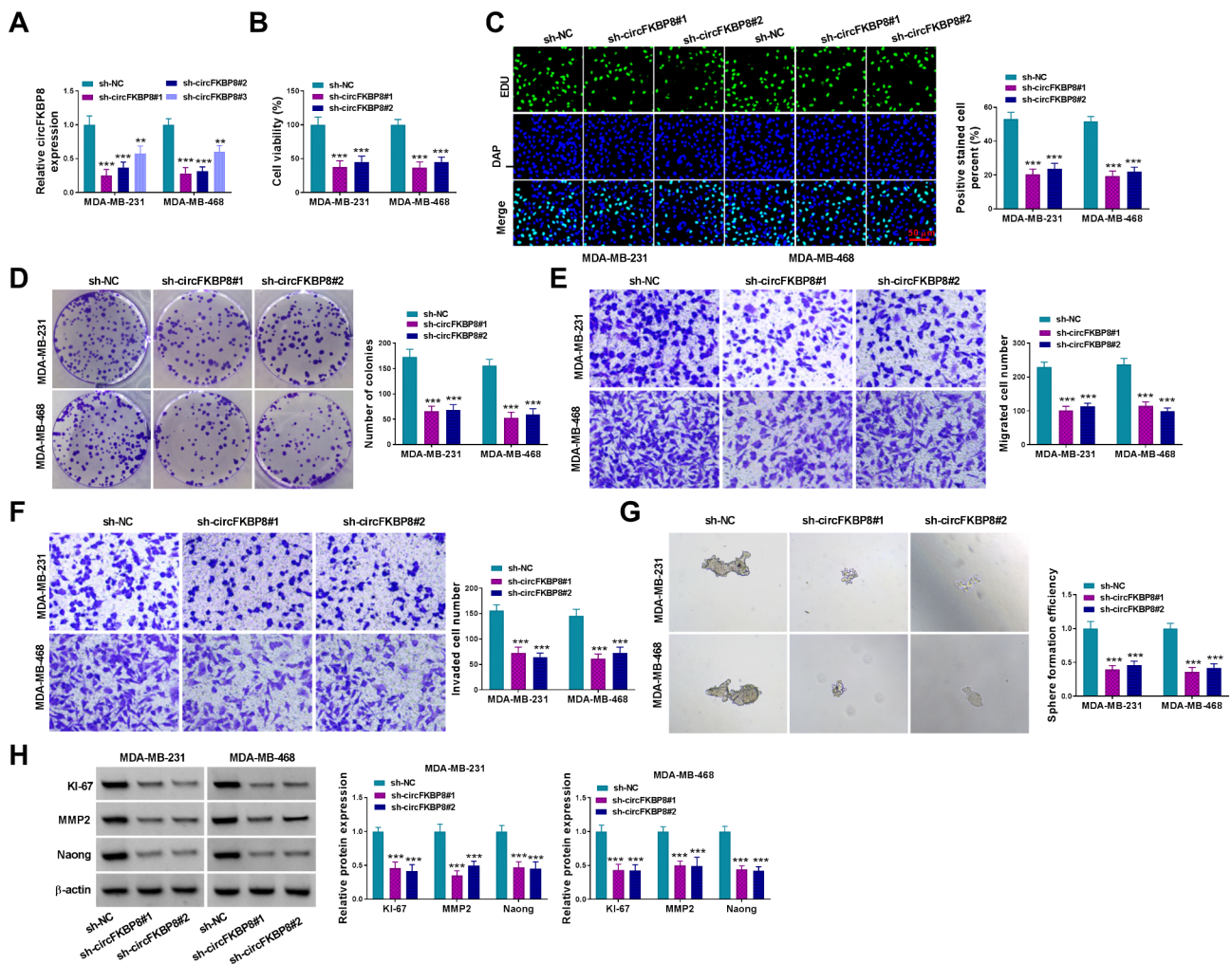


Fig. 2 CircFKBP8 inhibition suppressed BC cell proliferation, migration, invasion, and stemness. **(B)** The expression of circFKBP8 was detected after transfected with sh-NC, sh-circFKBP8#1, sh-circFKBP8#2, and sh-circFKBP8#3 in BC cells; **(B-D)** CCK-8 assay, EDU assay and colony formation assay were used to detect cell proliferation; **(E-F)** Transwell migration and invasion assays were performed to assess cell migration and invasion ability; **(G)** Sphere formation assay was used to evaluate cell stemness; **(H)** The protein levels of Ki-67, MMP2 and Nanog in BC cells were detected by western blot assays. ** $P < 0.01$, *** $P < 0.001$

Results

CircFKBP8 was significantly upregulated in BC tissues and cells

First, we found that circFKBP8 expression was significantly upregulated in BC tissues compared with adjacent non-cancer tissues (Fig. 1A), and circFKBP8 expression was notably increased in BC patients with distant metastasis compared with no metastasis (Fig. 1B). Survival analysis presented that high circFKBP8 expression in BC patients was significantly associated with a poor overall survival (OS) (Fig. 1C). CircFKBP8 expression was strikingly increased in MDA-MB-231, MDA-MB-453, BT549 and MDA-MB-468 BC cells compared to normal MCF10A cells (Fig. 1D). Because of the more significant upregulation of circFKBP8 in MDA-MB-231 and MDA-MB-468 BC cells ($P < 0.001$), we used the two cell lines in the subsequent experiments. RNase R treatment assay

demonstrated that circFKBP8 was more stable than the linear GAPDH mRNA when treatment with RNase R (Fig. 1E).

Knockdown of circFKBP8 inhibited BC cell proliferation, migration, invasion, and stemness

To explore the unknown functions of circFKBP8 in BC, we constructed circFKBP8 knockdown cells using three shRNAs targeting circFKBP8 (sh-circFKBP8#1, #2, and #3). According to the qRT-PCR results, three shRNAs could significantly reduce circFKBP8 expression, and sh-circFKBP8#1 had the highest knockdown efficiency (Fig. 2A). CCK8 assay showed that cell viability was inhibited in sh-circFKBP8#1 and sh-circFKBP8#2 groups relative to the sh-NC group (Fig. 2B). EDU and colony formation assays were used to detect BC cell proliferation. The results demonstrated that circFKBP8

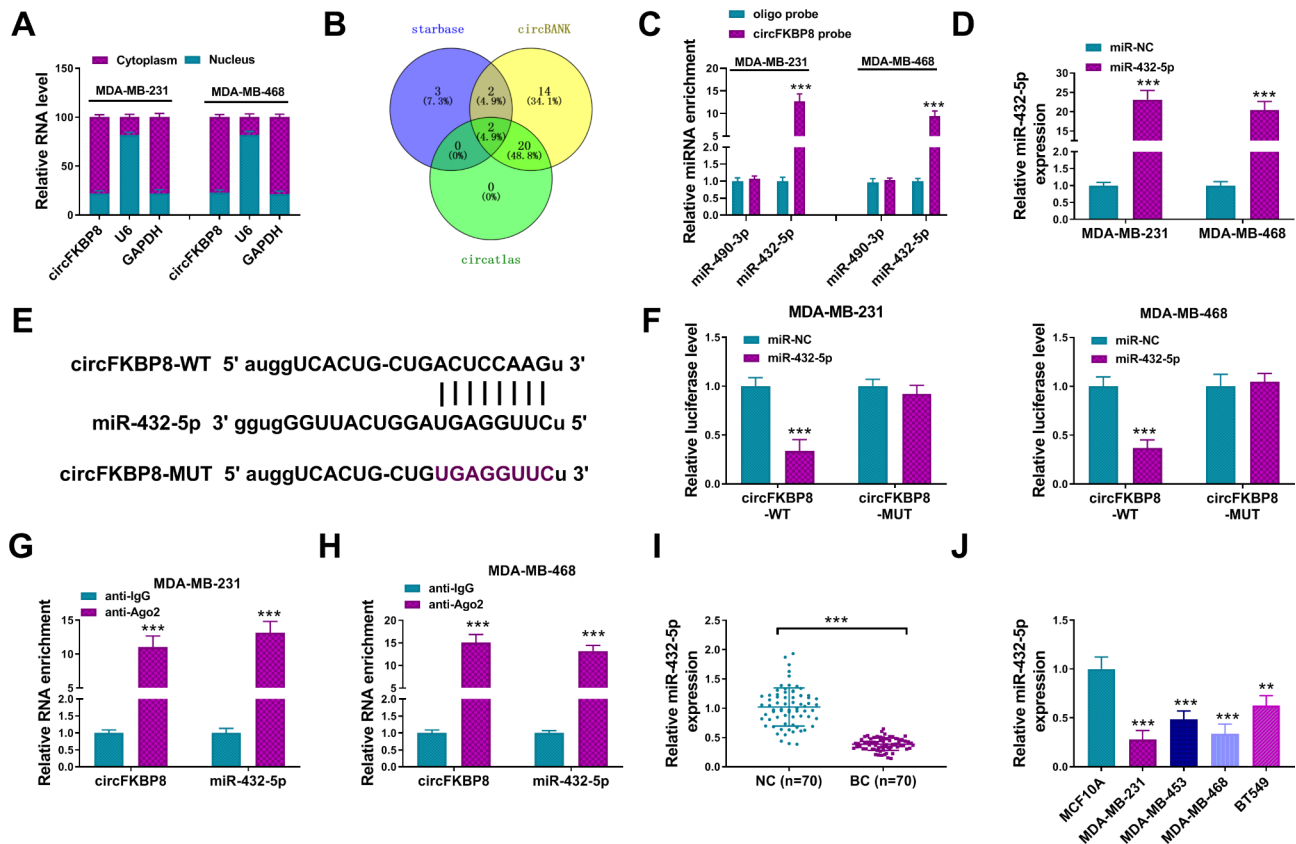


Fig. 3 CircFKBP8 bound to miR-432-5p in BC. **(A)** The nuclear and cytoplasmic fractions of circFKBP8 were detected by qRT-PCR in BC cells; **(B)** Prediction of downstream target miRNAs for circFKBP8 binding by bioinformatics websites (starbase, circBank, and circatlas); **(C)** The enrichment of miR-490-3p or miR-432-5p was detected by qRT-PCR after pull-down assay with oligo probe or circFKBP8 probe; **(D)** The expression of miR-432-5p was assessed after transfection with miR-432-5p or miR-NC. **(E)** Schematic diagram of binding sites between miR-432-5p and circFKBP8; **(F)** The luciferase activity was detected using dual-luciferase reporter assay after co-transfection with miR-NC or miR-432-5p and circFKBP8-WT or circFKBP8-MUT; **(G-H)** The enrichment of miR-432-5p and circFKBP8 was evaluated after immunoprecipitation with Ago2 in RIP assay; **(I-J)** miR-432-5p expression was detected in BC tissues and cells. ** $P < 0.01$, *** $P < 0.001$

knockdown reduced the percent of EdU-positive cells (Fig. 2C) and the number of generated colonies (Fig. 2D) in MDA-MB-231 and MDA-MB-468 cells. We also performed transwell assay, and found that inhibition of circFKBP8 greatly suppressed cell migration and invasion abilities (Fig. 2E-F). In addition, sphere formation assay was used to detect BC cell stemness. The results showed that depletion of circFKBP8 repressed MDA-MB-231 and MDA-MB-468 cell stemness ability (Fig. 2G). We also detected the protein levels of proliferation-related factor KI-67, invasion-related MMP2, and stemness-related protein Nanog in BC cells, and found that silencing of circFKBP8 significantly reduced the expression of KI-67, MMP2 and Nanog proteins (Fig. 2H). These data revealed that circFKBP8 knockdown inhibited BC cell malignant behaviors in vitro.

CircFKBP8 targeted miR-432-5p in BC

To explore the underneath mechanism of circFKBP8, we analyzed the location of circFKBP8 in BC cells. As

shown in Fig. 3A, circFKBP8 was mainly located in the cytoplasm of MDA-MB-231 and MDA-MB-468 cells. Increasing evidence suggested that circRNAs located in cytoplasm might function as sponges of miRNAs. The online tools circBank (<http://www.circbank.cn/index.html>), circatlas (http://www.geneseed.com.cn/page464?article_id=481) and starbase (<http://starbase.sysu.edu.cn>) were used to predict the target miRNAs of circFKBP8 and found two potential miRNAs (miR-490-3p and miR-432-5p) (Fig. 3B). RNA pull-down assay showed that miR-432-5p, but not miR-490-3p, was pulled down by the circFKBP8 probe (Fig. 3C). Then, miR-432-5p was used for the target research of circFKBP8. The data of qRT-PCR exhibited that miR-432-5p mimic transfection effectively induced overexpression of miR-432-5p compared with miR-NC transfection (Fig. 3D). To further demonstrate the relationship between miR-432-5p and circFKBP8, we performed dual-luciferase and RIP assays. According to the predicted binding site between miR-432-5p and circFKBP8, we constructed

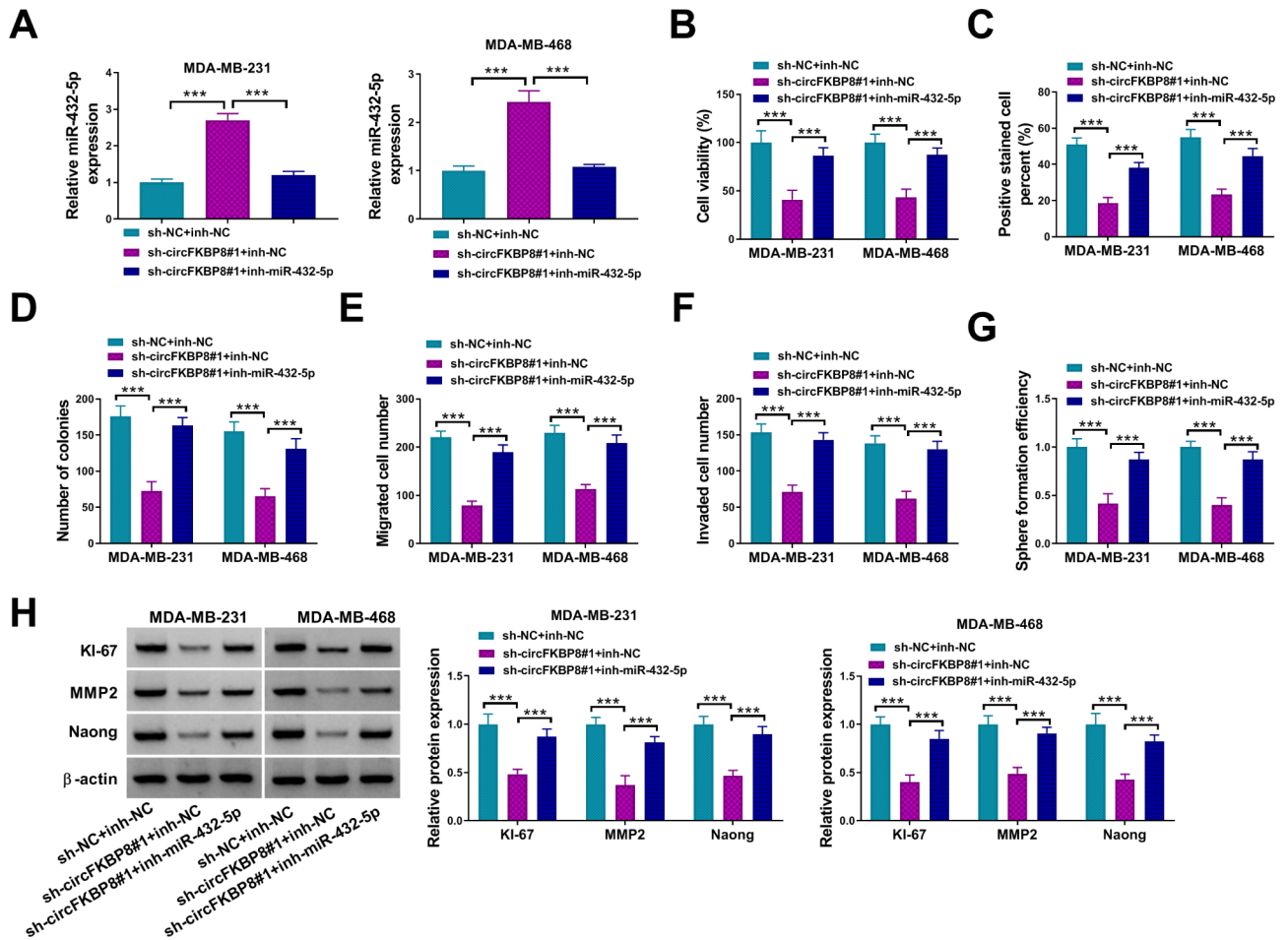


Fig. 4 MiR-432-5p inhibition rescued the effect of circFKBP8 knockdown on BC cell malignant behaviors. **(A-H)** MDA-MB-231 and MDA-MB-468 cells were transfected with sh-NC + inh-NC, sh-circFKBP8#1 + inh-NC, or sh-circFKBP8#1 + inh-miR-432-5p; **(A)** miR-432-5p expression was detected by qRT-PCR in MDA-MB-231 and MDA-MB-468 cells; **(B-D)** CCK8 assay, EDU assay and colony formation assay were used to assess cell proliferation; **(E-G)** Transwell assay and tube formation assay were performed to assess cell migration, invasion ability and stemness; **(H)** Western blot assay was performed to assess the protein levels of KI-67, MMP2 and Nanog. ****P* < 0.001

circFKBP8 WT and MUT reporter plasmids (Fig. 3E). The luciferase reporter activity showed that circFKBP8 could bind to miR-432-5p by the predicted binding site in MDA-MB-231 and MDA-MB-468 cells (Fig. 3F). The results of RIP assay suggested that the anti-Ago2 antibody could enrich circFKBP8 and miR-432-5p (Fig. 3G-H). Moreover, miR-432-5p expression was significantly reduced in BC tissues and cells (Fig. 3I-J). In addition, sh-circFKBP8#1 transfection dose-dependently elevated the amount of miR-432-5p in MDA-MB-231 and MDA-MB-468 cells (Supplementary Fig. 1). These data suggested that circFKBP8 functioned as a sponge of miR-432-5p in BC cells.

CircFKBP8 regulated BC cell progression by sponging miR-432-5p

To explore the regulatory axis between circFKBP8 and miR-432-5p in BC cells, different plasmids were transfected into BC cells. Silencing of circFKBP8 significantly

upregulated miR-432-5p expression, but miR-432-5p expression was partially downregulated by in-miR-432-5p (Fig. 4A). Depletion of miR-432-5p could reverse the inhibition in cell proliferation caused by circFKBP8 knockdown (Fig. 4B-D). Transwell migration and invasion assays showed that circFKBP8 knockdown inhibited cell migration and invasion, but the two impacts were restored by miR-432-5p inhibition (Fig. 4E-F). Suppression of circFKBP8 inhibited cell stemness, while miR-432-5p inhibitor recovered the impact (Fig. 4G). Moreover, circFKBP8 knockdown reduced KI-67, MMP2 and Naog protein levels, whereas miR-432-5p inhibition restored the impacts (Fig. 4H). These data suggested that circFKBP8 regulated BC cell progression by sponging miR-432-5p.

MiR-432-5p targeted E2F7 in BC

Starbase algorithm predicted that E2F7 was a possible downstream target of miR-432-5p (Fig. 5A).

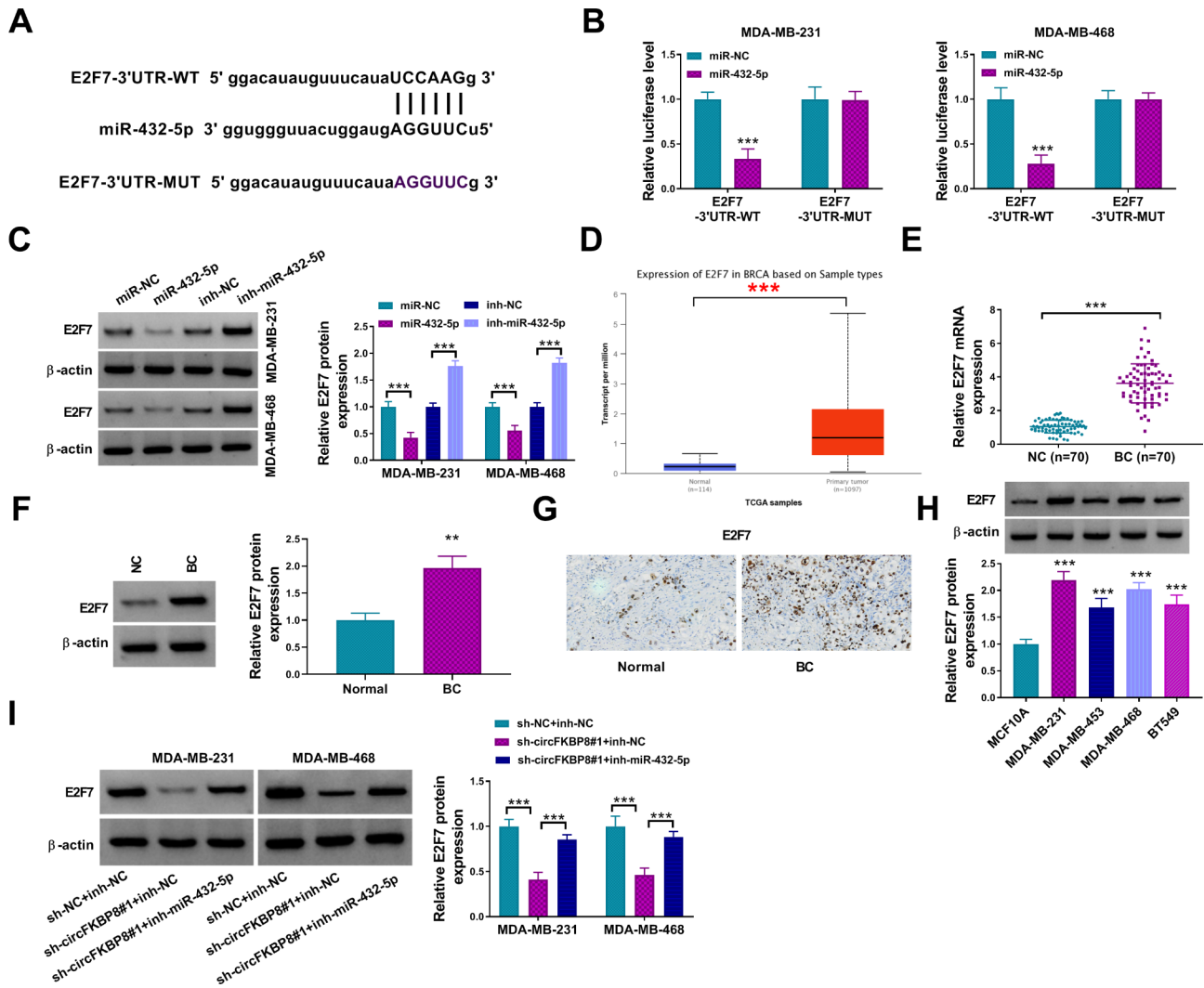


Fig. 5 E2F7 was a direct target of miR-432-5p. (A) The binding sites were predicted by starbase between miR-432-5p and E2F7; (B) Luciferase activity was detected in dual-luciferase assay; (C) The protein expression of E2F7 was detected in different groups; (D) UALCAN was used to analyze E2F7 expression in BC tissues in TCGA database; (E-G) The mRNA (E) and protein (F-G) levels of E2F7 in BC tissues were analyzed by qRT-PCR and western blot/IHC assays; (H) Western blot was used for protein analysis of E2F7 in BC cells; (I) After BC cells were transfected with sh-NC + inh-NC, sh-circFKBP8#1 + inh-NC, or sh-circFKBP8#1 + inh-miR-432-5p, the protein level of E2F7 was detected. ** $P < 0.01$, *** $P < 0.001$

Dual-luciferase reporter assays revealed that miR-432-5p could bind to E2F7-3'UTR to target E2F7 (Fig. 5B). Western blot results revealed that miR-432-5p overexpression downregulated E2F7 expression, while miR-432-5p inhibition elevated E2F7 protein level (Fig. 5C). In addition, we analyzed TCGA datasets through UALCAN tool, and found that E2F7 was strikingly increased in BC tissues ($n=1097$) relative to normal tissues ($n=114$) (Fig. 5D). Furthermore, E2F7 mRNA (Fig. 5E) and protein (Fig. 5F-G) levels were notably upregulated in BC tissues compared to normal controls. Also, the protein expression of E2F7 was higher in BC cells than that in normal MCF10A cells (Fig. 5H). Moreover, circFKBP8 suppression decreased E2F7 protein expression, while co-transfection with miR-432-5p inhibitor partially increased

E2F7 protein expression (Fig. 5I). These data suggested that miR-432-5p directly targeted E2F7 in BC.

E2F7 knockdown suppressed BC cell proliferation, migration, invasion, and stemness

To further explore the role of E2F7 in BC, the si-E2F7 was used to knock down E2F7. E2F7 protein level was drastically reduced in MDA-MB-231 and MDA-MB-468 cells transfected with si-E2F7 (Fig. 6A). After E2F7 downregulation, the proliferation, migration, invasion and stemness of MDA-MB-231 and MDA-MB-468 cell were evidently inhibited (Fig. 6B-G). In addition, E2F7 inhibition significantly decreased KI-67, MMP2 and Nanog protein levels in MDA-MB-231 and MDA-MB-468 cells

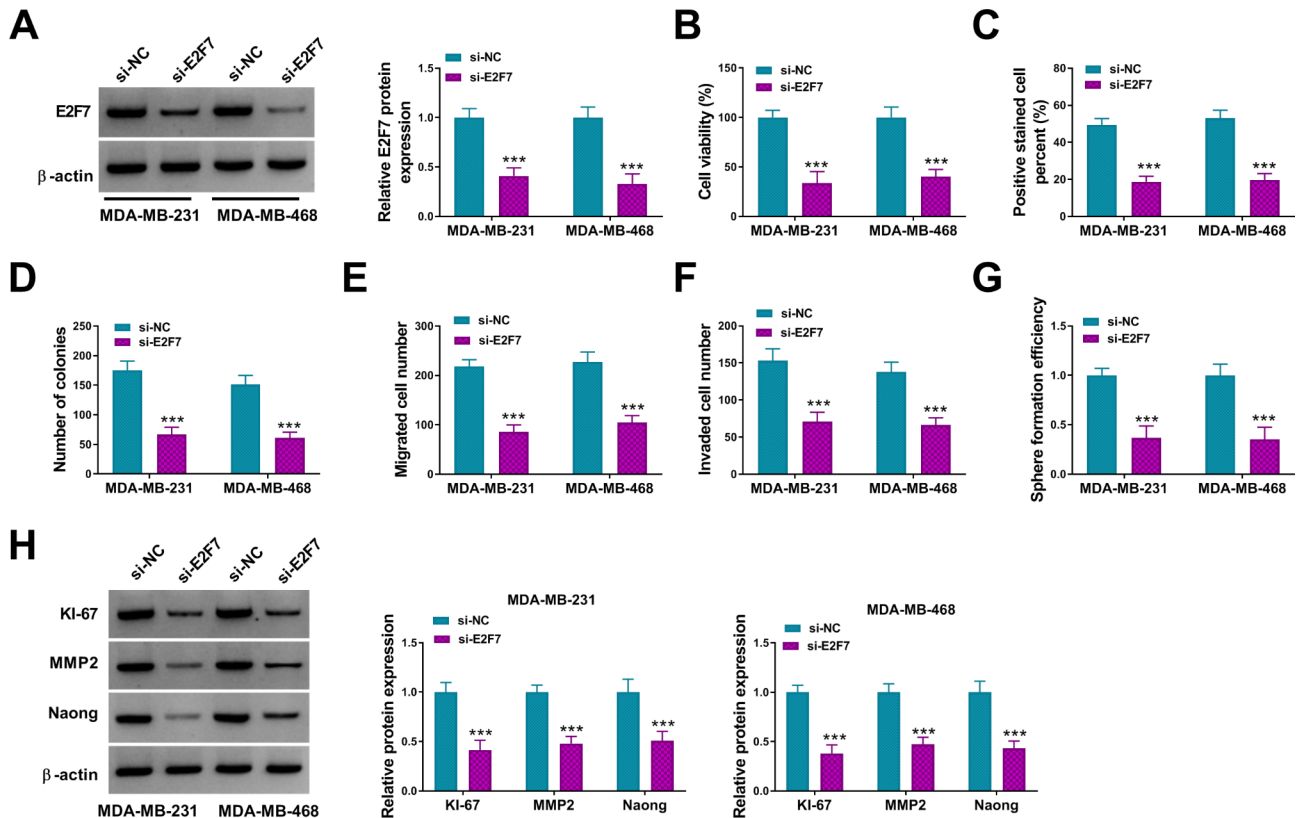


Fig. 6 E2F7 promoted BC cell proliferation, migration, invasion, and stemness. MDA-MB-231 and MDA-MB-468 cells were transfected with si-NC or si-E2F7. **(A)** The protein level of E2F7 was detected after knockdown of E2F7 in BC cells; **(B–G)** CCK-8 assay, EDU assay, colony formation assay, transwell migration and invasion assay, and sphere formation assay were used to detect cell proliferation, migration and invasion ability and cell stemness; **(H)** Western blot assay was used to detect the protein levels of KI-67, MMP2 and Nanog in BC cells. *** $P < 0.001$

(Fig. 6H). These data indicated that E2F7 could promote BC cell malignant behaviors.

MiR-432-5p suppressed BC cells progression via downregulating E2F7

Considering the relationship between miR-432-5p and E2F7, rescued experiments were performed in BC cells. MiR-432-5p overexpression inhibited E2F7 protein level, while cotransfection of the E2F7 overexpression plasmid partially increased E2F7 protein expression (Fig. 7A). Overexpression of miR-432-5p suppressed the proliferation, migration, invasion and stemness of MDA-MB-231 and MDA-MB-468 cells, which could be reversed by increased E2F7 expression (Fig. 7B–G). Moreover, overexpression of E2F7 restored miR-432-5p mimic-mediated reduction in KI-67, MMP2 and Nanog protein levels (Fig. 7H). These data suggested that miR-432-5p repressed the proliferation, migration, invasion, and stemness by regulating E2F7 expression in BC cells.

CircFKBP8 promoted BC tumor growth in vivo

Xenograft assays were used to study the role of circFKBP8 on tumor growth in vivo. After knockdown of circFKBP8, tumor volume and weight were remarkably reduced

(Fig. 8A–B). The expression of E2F7, MMP2 and Nanog was decreased in tumor tissues with sh-circFKBP8#1 transduction (Fig. 8C). Moreover, the tumors with sh-circFKBP8#1 transduction had fewer KI-67-positive cells (Fig. 8C). After sh-circFKBP8#1 transduction, the expression of circFKBP8 and E2F7 mRNA was remarkably decreased, but miR-432-5p expression was increased in tumor tissues (Fig. 8D). In addition, circFKBP8 silencing significantly inhibited the protein levels of E2F7, KI-67, MMP2 and Nanog in tumor tissues (Fig. 8E). These data demonstrated that circFKBP8 functioned as an oncogenic circRNA to promote BC tumor growth.

Discussion

BC is the most prevalent malignancy [14] and the second leading cause of cancer death in women worldwide [15]. Therefore, it is critical to identify promising therapeutic targets for BC treatment.

Increasing evidence suggests that circRNAs are involved in cancer progression [16–19]. For example, circ_0008035 accelerated proliferation and migration of gastric cancer cells [20]. CircCYP24A1 impeded tumorigenesis, cell migration and invasion of renal cell carcinoma [21]. Also, circRNA_002178 knockdown was

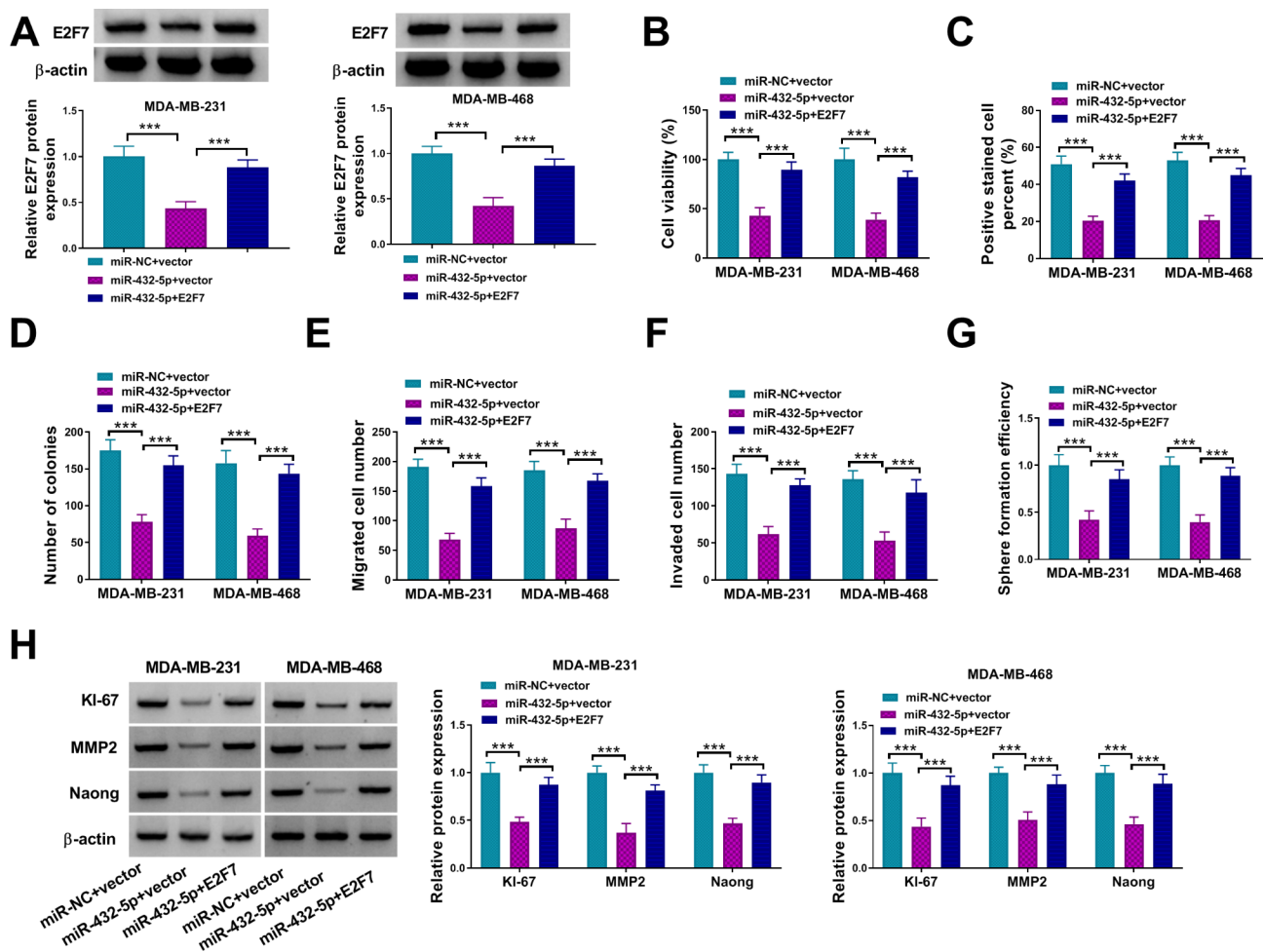


Fig. 7 MiR-432-5p inhibited BC cells malignant behaviors by negatively regulating E2F7 expression. **(A–H)** MDA-MB-231 and MDA-MB-468 cells were transfected with miR-NC + vector, miR-432-5p + vector or miR-432-5p + E2F7; **(A)** Western blot analysis was used to evaluate the protein level of E2F7 in BC cells; **(B–F)** The proliferation, migration invasion, and stemness of BC cells were detected by CCK8 assay, EDU assay, colony formation assay, transwell migration and invasion assay, and sphere formation assay, respectively; **(G)** The Ki-67, MMP2 and Nanog protein levels were detected in MDA-MB-231 and MDA-MB-468 cells by western blot assays. *** $P < 0.001$

shown to suppress malignant phenotypes of BC cells [22]. In our study, circFKBP8 was upregulated in BC tissues and cells. CircFKBP8 inhibition suppressed BC cell proliferation, migration, invasion, and stemness. Thus, circFKBP8 could promote malignant behaviors of BC cells in vitro. In addition, silencing of circFKBP8 limited tumor growth in vivo. These results together demonstrated that circFKBP8 acted as an oncogenic factor in BC.

CircRNAs are reported as important regulators in various cancers by acting as sponges of certain miRNAs to mitigate the inhibition of miRNAs on their downstream genes [23–25]. MiR-432-5p repressed colorectal cancer cell growth and invasion through regulating CXCL5 expression [26]. MiR-432-5p inhibited BC cell progression by targeting SLBP [27]. In our study, we demonstrated that miR-432-5p was significantly reduced in BC. MiR-432-5p inhibition restored the suppression effects

of circFKBP8 knockdown on BC cell malignant behaviors, indicating that miR-432-5p was a tumor suppressor in BC. The oncogenic function of circFKBP8 may be, at least in part, achieved by miR-432-5p reduction.

E2F7 is a known transcriptional factor and acts as a tumor promoter in various cancer [28, 29]. Overexpression of E2F7 promoted BC cell proliferation [30]. Consistent with the previous study, our data showed that knockdown of E2F7 suppressed cell malignant progression in BC. Furthermore, E2F7 was confirmed as a downstream target of miR-432-5p, and overexpression of E2F7 could rescue anti-tumor activity of miR-432-5p overexpression in BC cells. Thus, E2F7 promoted BC cell progression, and miR-432-5p functioned as a tumor inhibitor in BC via targeting E2F7. The circRNA/miRNA/mRNA axis has been researched in BC progression, such as circ_0103552/miR-515-5p/CYR61 and circ_000554/miR-182/ZFP36 networks [31, 32]. Herein, we found that

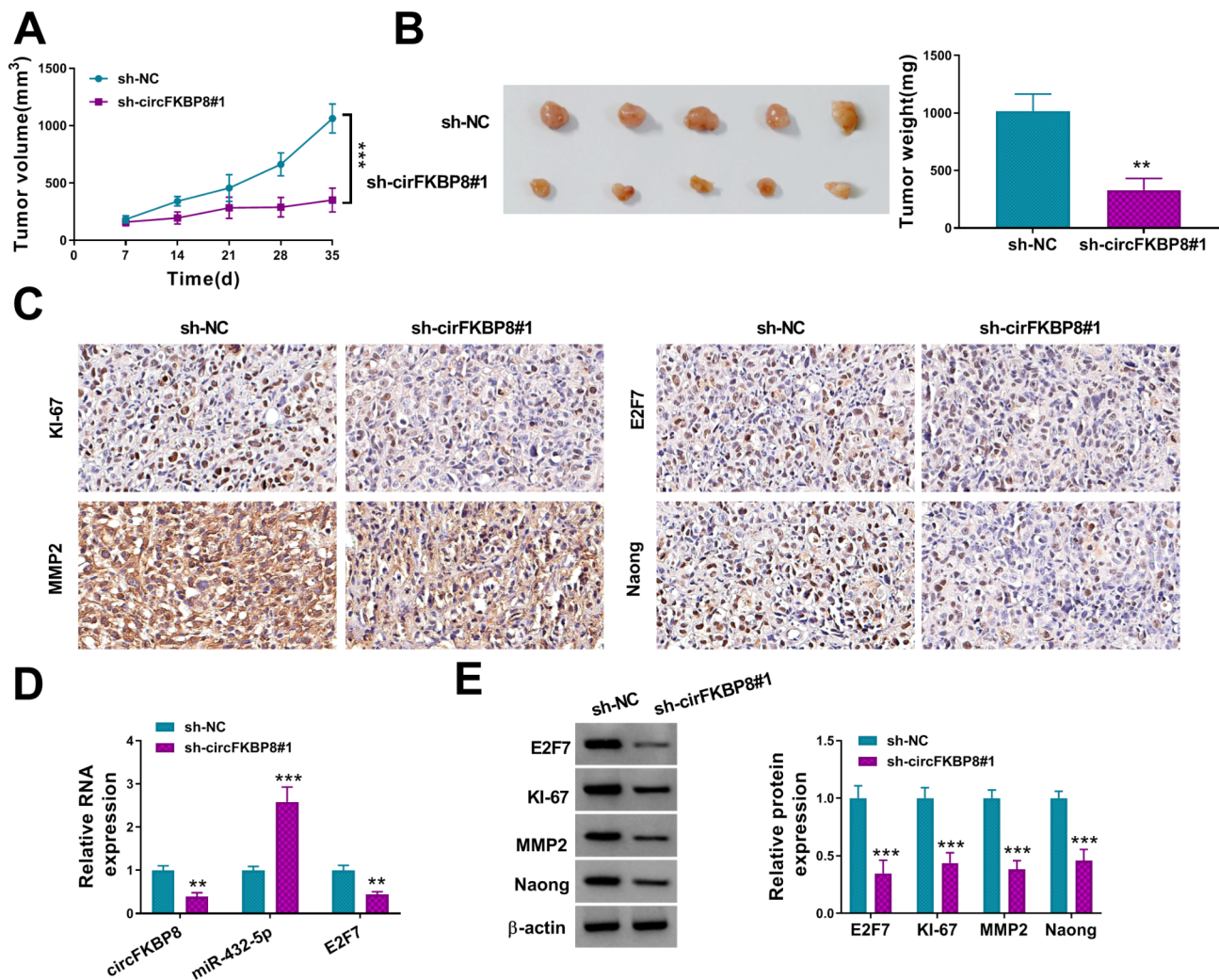


Fig. 8 CircFKBP8 knockdown inhibited BC tumor growth in vivo. Xenograft model of sh-NC or sh-circFKBP8#1 group was established in mice. **(A-B)** Tumor volume and Tumor weight were detected in Xenograft assay; **(C)** The levels of Ki-67, E2F7, MMP2 and Nanog was assessed by IHC staining in different groups; **(D)** The expression of circFKBP8, miR-432-5p and E2F7 was detected by qRT-PCR in tumors from different groups; **(E)** The protein levels of Ki-67, E2F7, MMP2 and Nanog were evaluated by western blot assays in tumors from different groups. ** $P < 0.01$, *** $P < 0.001$

circFKBP8 downregulation resulted in E2F7 inhibition via releasing miR-432-5p in BC cells. Then, we concluded that circFKBP8 could regulate BC progression via targeting the miR-432-5p/E2F7 axis.

To sum up, our in vitro and in vivo data suggested that circFKBP8 functioned as an oncogenic factor in BC by sponging miR-432-5p to upregulate E2F7 expression. Our findings suggest that circFKBP8 could serve as a novel therapeutic target for BC treatment.

Supplementary Information

The online version contains supplementary material available at <https://doi.org/10.1186/s41065-024-00331-1>.

Supplementary Material 1: Supplementary Fig. 1 Impact of sh-circFKBP8#1 on miR-432-5p expression in MDA-MB-231 and MDA-MB-468 cells by qRT-PCR. * $P < 0.05$, ** $P < 0.01$, *** $P < 0.001$.

Acknowledgements

Not applicable.

Author contributions

Conceptualization and Methodology: Wang Xu, Kunlin Yu and Changshan Liu; Formal analysis and Data curation: Cailu Luo, Xiaodan Luo and Tao Lian; Validation and Investigation: Zhongkui Jin, Changshan Liu and Wang Xu; Writing - original draft preparation and Writing - review and editing: Zhongkui Jin, Wang Xu, and Kunlin Yu; Approval of final manuscript: all authors.

Funding

No funding was received.

Data Availability

The analyzed data sets generated during the present study are available from the corresponding author on reasonable request.

Declarations

Ethics approval and consent to participate

The present study was approved by the ethical review committee of Yichun People's Hospital & The Affiliated Yichun Hospital of Nanchang University. Written informed consent was obtained from all enrolled patients.

Consent for publication

Patients agree to participate in this work.

Competing interests

The authors declare that they have no competing interests.

Received: 18 December 2023 / Accepted: 12 August 2024

Published online: 27 August 2024

References

- Ginsburg O, Bray F, Coleman M, Vanderpuye V, Eniu A, Kotha S, Sarker M, Huang T, Allemani C, Dvaladze A, Gralow J, Yeates K, Taylor C, Oomman N, Krishnan S, Sullivan R, Kombe D, Blas M, Parham G, Kassami N, Conteh L. The global burden of women's cancers: a grand challenge in global health. *Lancet* (London England). 2017;389:847–60. [https://doi.org/10.1016/s0140-6736\(16\)31392-7](https://doi.org/10.1016/s0140-6736(16)31392-7).
- Siegel R, Miller K, Jemal A. Cancer statistics, 2017. *Cancer J Clin*. 2017;67:7–30. <https://doi.org/10.3322/caac.21387>.
- Li T, Mello-Thoms C, Brennan P. Descriptive epidemiology of breast cancer in China: incidence, mortality, survival and prevalence. *Breast Cancer Res Treat*. 2016;159:395–406. <https://doi.org/10.1007/s10549-016-3947-0>.
- Kristensen L, Andersen M, Stagsted L, Ebbesen K, Hansen T, Kjems J. The biogenesis, biology and characterization of circular RNAs. *Nat Rev Genet*. 2019;20:675–91. <https://doi.org/10.1038/s41576-019-0158-7>.
- Li X, Yang L, Chen L. The Biogenesis, functions, and challenges of Circular RNAs. *Mol Cell*. 2018;71:428–42. <https://doi.org/10.1016/j.molcel.2018.06.034>.
- Arnaiz E, Sole C, Manterola L, Iparraguirre L, Otaegui D, Lawrie C. CircRNAs and cancer: biomarkers and master regulators. *Sem Cancer Biol*. 2019;58:90–9. <https://doi.org/10.1016/j.semcancer.2018.12.002>.
- Chen Y, Xu S, Liu X, Jiang X, Jiang J. CircSEC24A upregulates TGFBR2 expression to accelerate pancreatic cancer proliferation and migration via sponging to miR-606. *Cancer Cell Int*. 2021;21:671. <https://doi.org/10.1186/s12935-021-02392-y>.
- Dong X, Zhang P, Liu L, Li H, Cheng S, Li S, Wang Y, Zheng C, Dong J, Zhang L. The Circ_0001367/miR-545-3p/LUZP1 Axis regulates Cell Proliferation, Migration and Invasion in Glioma cells. *Front Oncol*. 2021;11:781471. <https://doi.org/10.3389/fonc.2021.781471>.
- Xu X, Wang S, Wang H, Pan C, Yang W, Yu J. Hsa_circ_0008434 regulates USP9X expression by sponging miR-6838-5p to promote gastric cancer growth, migration and invasion. *BMC Cancer*. 2021;21:1289. <https://doi.org/10.1186/s12885-021-09052-4>.
- Wan L, Han Q, Zhu B, Kong Z, Feng E. Circ-TFF1 facilitates breast Cancer Development via Regulation of miR-338-3p/FGFR1 Axis. *Biochem Genet*. 2021. <https://doi.org/10.1007/s10528-021-10102-6>.
- Zhong W, Bao L, Yuan Y, Meng Y. CircRASSF2 acts as a prognostic factor and promotes breast cancer progression by modulating miR-1205/HOXA1 axis. *Bioengineered*. 2021;12:3014–28. <https://doi.org/10.1080/21655979.2021.1933300>.
- Gong G, She J, Fu D, Zhen D, Zhang B. Circular RNA circ_0084927 regulates proliferation, apoptosis, and invasion of breast cancer cells via miR-142-3p/ERC1 pathway. *Am J Translational Res*. 2021;13:4120–36.
- Yang R, Xing L, Zheng X, Sun Y, Wang X, Chen J. The circRNA circAGFG1 acts as a sponge of miR-195-5p to promote triple-negative breast cancer progression through regulating CCNE1 expression. *Mol Cancer*. 2019;18:4. <https://doi.org/10.1186/s12943-018-0933-7>.
- Bray F, Ferlay J, Soerjomataram I, Siegel R, Torre L, Jemal A. Global cancer statistics 2018: GLOBOCAN estimates of incidence and mortality worldwide for 36 cancers in 185 countries. *Cancer J Clin*. 2018;68:394–424. <https://doi.org/10.3322/caac.21492>.
- DeSantis C, Ma J, Gaudet M, Newman L, Miller K, Goding Sauer A, Jemal A, Siegel R. Breast cancer statistics, 2019. *Cancer J Clin*. 2019;69:438–51. <https://doi.org/10.3322/caac.21583>.
- Xie Y, Hang X, Xu W, Gu J, Zhang Y, Wang J, Zhang X, Cao X, Zhan J, Wang J, Gan J. CircFAM13B promotes the proliferation of hepatocellular carcinoma by sponging miR-212, upregulating E2F5 expression and activating the P53 pathway. *Cancer Cell Int*. 2021;21:410. <https://doi.org/10.1186/s12935-021-02120-6>.
- Xiong H, Yu J, Jia G, Su Y, Zhang J, Xu Q, Sun X. Emerging roles of circU-BAP2 targeting miR-370-3p in proliferation, apoptosis, and invasion of papillary thyroid cancer cells. *Hum Cell*. 2021. <https://doi.org/10.1007/s13577-021-00585-1>.
- Xu Y, Zhao J, Gao C, Ni X, Wang W, Hu W, Wu C. Hsa_circ_0136666 activates Treg-mediated immune escape of colorectal cancer via miR-497/PD-L1 pathway. *Cell Signal*. 2021;110095. <https://doi.org/10.1016/j.cellsig.2021.110095>.
- Zhang X, Li X, Fu X, Yu M, Qin G, Chen G, Huang C. Circular RNA TAF4B promotes bladder Cancer progression by sponging miR-1298-5p and regulating TGFA expression. *Front Oncol*. 2021;11:643362. <https://doi.org/10.3389/fonc.2021.643362>.
- Chu C, Liu X, Zhao Z, Shi Z. Circ_0008035 promotes the progression of gastric cancer via the regulation of miR-1256/CEACAM6 axis. *Cell Cycle*. 2022;1–12. <https://doi.org/10.1080/15384101.2022.2041354>.
- Wu X, Zhou J, Zhao L, Yang Z, Yang C, Chen Y, Xue W. CircCYP24A1 hampered malignant phenotype of renal cancer carcinoma through modulating CMTM-4 expression via sponging miR-421. *Cell Death Dis*. 2022;13:190. <https://doi.org/10.1038/s41419-022-04623-0>.
- Liu T, Ye P, Ye Y, Lu S, Han B. Circular RNA hsa_circRNA_002178 silencing retards breast cancer progression via microRNA-328-3p-mediated inhibition of COL1A1. *J Cell Mol Med*. 2020;24:2189–201. <https://doi.org/10.1111/jcmm.14875>.
- Liu B, Tian Y, Chen M, Shen H, Xia J, Nan J, Yan T, Wang Y, Shi L, Shen B, Yu H, Cai X. CircUBAP2 promotes MMP9-Mediated oncogenic effect via sponging miR-194-3p in Hepatocellular Carcinoma. *Front cell Dev Biology*. 2021;9:675043. <https://doi.org/10.3389/fcell.2021.675043>.
- Ma G, Li G, Fan W, Xu Y, Song S, Guo K, Liu Z. Circ-0005105 activates COL11A1 by targeting miR-20a-3p to promote pancreatic ductal adenocarcinoma progression. *Cell Death Dis*. 2021;12:656. <https://doi.org/10.1038/s41419-021-03938-8>.
- Zhou J, Wang L, Sun Q, Chen R, Zhang C, Yang P, Tan Y, Peng C, Wang T, Jin C, Ji J, Jin K, Sun Y. Hsa_circ_0001666 suppresses the progression of colorectal cancer through the miR-576-5p/PCDH10 axis. *Clin Translational Med*. 2021;11:e565. <https://doi.org/10.1002/ctm2.565>.
- Luo M, Hu Z, Kong Y, Li L. MicroRNA-432-5p inhibits cell migration and invasion by targeting CXCL5 in colorectal cancer. *Experimental Therapeutic Med*. 2021;21:301. <https://doi.org/10.3892/etm.2021.9732>.
- Li S, Jia H, Zhang Z, Wu D. DRAC1 promotes growth of breast cancer by sponging miR-432-5p to upregulate SLBP. *Cancer Gene Ther*. 2021. <https://doi.org/10.1038/s41417-021-00388-4>.
- Wang Y, Wo Y, Lu T, Sun X, Liu A, Dong Y, Du W, Su W, Huang Z, Jiao W. Circ-AA5DH functions as the progression of early stage lung adenocarcinoma by targeting miR-140-3p to activate E2F7 expression. *Translational lung cancer Res*. 2021;10:57–70. <https://doi.org/10.21037/tlcr-20-1062>.
- Zhou P, Xiao L, Xu X. Identification of E2F transcription factor 7 as a novel potential biomarker for oral squamous cell carcinoma. *Head Face Med*. 2021;17:7. <https://doi.org/10.1186/s13005-021-00258-2>.
- Liu J, Li X, Wang M, Xiao G, Yang G, Wang H, Li Y, Sun X, Qin S, Du N, Ren H, Pang Y. A miR-26a/E2F7 feedback loop contributes to tamoxifen resistance in ER-positive breast cancer. *Int J Oncol*. 2018;53:1601–12. <https://doi.org/10.3892/ijo.2018.4492>.
- Huang Q, He Y, Zhang X, Guo L. Circular RNA hsa_circ_0103552 promotes proliferation, Migration, and Invasion of breast Cancer cells through Upregulating Cysteine-Rich angiogenic inducer 61 (CYR61) expression via sponging MicroRNA-515-5p. *Tohoku J Exp Med*. 2021;255:171–81. <https://doi.org/10.1620/tjem.255.171>.
- Mao Y, Lv M, Cao W, Liu X, Cui J, Wang Y, Wang Y, Nie G, Liu X, Wang H. Circular RNA 000554 represses epithelial-mesenchymal transition in breast cancer by regulating microRNA-182/ZFP36 axis. *FASEB J*. 2020;34:11405–20. <https://doi.org/10.1096/fj.201903047R>.

Publisher's note

Springer Nature remains neutral with regard to jurisdictional claims in published maps and institutional affiliations.